Enhanced propagation in a plasmonic chain waveguide with nanoshell structures based on low- and high-order mode coupling

Xudong Cui* and Daniel Erni

General and Theoretical Electrical Engineering (ATE), Faculty of Engineering, University of Duisburg-Essen, Campus Duisburg, D-47048 Duisburg, Germany
**Corresponding author: xudong.cui@uni-due.de*

Received February 1, 2008; revised May 9, 2008; accepted May 12, 2008;
posted May 13, 2008 (Doc. ID 92362); published June 26, 2008

We studied the performance of a plasmonic chain waveguide by employing an array of nanoshell structures. The optical properties of the proposed structures are discussed in detail with respect to the mode coupling for both low-order resonances and high-order multipolar modes. We show (a) that the choice of nanoshell particles allows an easy tuning of the structure's resonances according to given wavelength specifications and (b) that the resonances are insensitive to the chain length when high-order multipolar modes are involved. Moreover, chain waveguides that are operated on resonant multipolar modes provide propagation lengths up to 1.88 μm, which is beyond what is maximally achieved by conventional solid particle chains. This is attributed to the large field enhancement within metallic nanoshell structures, as well as to far-field effects, which play an important role in low-loss light guiding along nanoshell chains. © 2008 Optical Society of America

OCIS codes: 230.0230, 230.3120, 230.7370, 240.6680, 290.5850.

1. INTRODUCTION

Light confinement below the optical diffraction limit can be achieved by employing tightly guided propagation states such as surface plasmon polaritons (SPPs) or resonant states based on localized surface plasmons (LSPs), both carried by highly dispersive metallodielectric structures in the nanoscale [1]. Recently, several structures have been proposed and demonstrated for light guiding to subwavelength dimensions, i.e., metal strips [2], nanowires [3], V-groove channel/wedge waveguides [4], and nanoparticle chains [5,6]. Among these structures, nanoparticle chain waveguides are particularly attractive because they provide a strong 3D mode confinement [5–7]. Coherent light propagation along a linear chain of solid metallic nanoparticles has been demonstrated to support propagation distances up to hundreds of nanometers [5–8]. Here a large field confinement to nanoscopic length scales is provided only when the underlying particles are operated at their resonance wavelengths. Chain waveguides based on the coupling of low-order (dipole) modes turned out to be sensitive to the overall structure lengths, providing a setting that is barely controllable within a proper waveguide design. Moreover, the propagation length in such structures is usually much shorter than in alternative metallic waveguide topologies owing to the large material losses and the radiation damping of the coupled localized plasmon resonances [5]. Therefore a feasible means to control both the losses and the mesoscopic nature of such finite-length particle chains may become highly desirable.

Recent research has shown that resonant excitation of larger metallic particles (i.e., the particle dimensions are much larger than the wavelength of light) or even aspherical particles gives rise to broad extinction spectra with significant contributions from higher-order multipolar modes [9,10]. Although these modes have distinct far-field and spectral signatures, multipolar mode coupling is mostly ignored, and particularly in the context of nanoparticle chain waveguides. This is because solid spherical particles hardly support high-order resonances when the particle sizes are much less than the operating wavelength.

The appearance of nanoshell structures provided us with the possibility to excite different order modes even within spherical geometries [10]. Because of the wide tuning range of surface plasmon resonances (SPRs), nanoshells have been widely used for biosensors [11], as well as for nonlinear plasmon-based functional devices for ultra-low-power switching and optical limiting [12].

One promising feature of nanoshell structures is that optical properties such as the absorption can be altered according to a proper choice of particle dimensions and material parameters [13]. Therefore, it was expected that the use of nanoshell particles may provide additional degrees of freedom for the design of chain waveguides compared to their solid metallic counterparts.

The remainder of the paper is organized as follows. In Section 2, a brief description of the involved numerical simulation method is provided together with a discussion of the proper excitation condition for the involved plasmon modes, which then leads to the setup of a generic chain waveguide model. Section 3 starts with the analysis of single nanoshell structures and evolves into the full-wave simulation of nanoshell chain waveguides, including detailed studies of transmission characteristics in the light of dipole and multipolar mode coupling. The latter

enables tunable chain waveguide structures with particle resonances that are nearly insensitive to the chain length. Specific mechanisms in support of large propagation lengths are discussed at the end of this section. Finally, in Section 4 conclusions are drawn based on our numerical results.

2. NUMERICAL MODELS

Our simulations were carried out with the commercial software package COMSOL, which includes a computational electromagnetic code based on the finite element method (FEM) [14]. Scattering boundary conditions (SBCs) and perfectly matched layers (PMLs) are combined together to properly define the computational window: First, SBCs are put at least half of the maximal incident wavelength apart from the structure to absorb the scattering waves impinging on the truncated boundaries. Second, the PMLs are then consecutively added outside the SBCs to efficiently absorb spurious reflections from the SBCs.

Since the plasmon resonances of most bulk noble metals are in the visible and ultraviolet wavelength range, our calculations are thus carried out for wavelengths around 300 nm–700 nm. In our model, we have used the well-established measured data set for the material dispersion of silver according to Johnson and Christy [15]. Further material model corrections due to the finite electron mean free path in the nanoparticles are not taken into account since the minimal size of metallic particles in our work is larger than 5 nm, and it is generally believed that the bulk material properties of metals are still valid in such length scales [16].

Because of the huge computational resources required for the 3D simulation of spherical nanoshells, only 2D cylindrical structures are considered in this work. Due to the polarization selectivity of the plasmon excitation, all simulations are carried out for p polarization, where the magnetic field is parallel to the cylinder axis.

In experimental settings the use of the scanning near-field optical microscopy (SNOM) tip has proved to be highly efficient in order to excite the plasmon modes within nanoparticles [17]. This is mainly because of the near field that surrounds the SNOM tip, where its evanescent components are capable of exciting surface plasmons. However, it was also observed that the propagation length of the chain waveguide may become sensitive to the launching conditions, such as the tip height and the size of the probe aperture, rendering any investigation highly context dependent [18]. In the case of single metal nanoparticles, LSPs are excited by light absorption in the nanoparticles. Therefore, no special geometries, such as those required for the excitation of. e.g., SPRs along a planar metal–dielectric interface [9], are used here. In our simulations we use plane waves or point dipoles as excitation sources. Simple plane-wave excitation is best suited for obtaining the resonances of the structures, while point dipole or multipole sources are applied to mimick the experimental cases when we determine the propagation length of the chain waveguides. In particular, transversely (T) polarized wave propagation (T wave) and longitudinally (L) polarized wave propagation (L wave) are considered here to analyze the specific coupling behaviors. It should be noted that the T and L waves are uncoupled, whereas all other forms of propagating fields can be described as a linear combination of the two mode types. In this paper, we will focus only on the case when the interparticle separation is much less than the diameter of the particle.

3. RESULTS AND DISCUSSION

A. Optical Properties of a Single Nanoshell

For a single nanoshell, the SPRs can be obtained analytically by the extended Mie theory within the quasi-static approximation [9]. Here we used the numerical method to investigate the SPRs for different nanoshells based on the scattering cross section (SCS) of the particle. The SCS is defined from the scattered and incident field via Poynting's vector, and it is essentially the ratio of the outgoing radial flux to the incoming flux associated with the plane-wave solution. Three structures are considered, namely, a pure metallic rod (structure #1), a dielectric nanoshell consisting of an Ag core and a dielectric coating (structure #2), and a metallic nanoshell with a dielectric core and an Ag coating (structure #3). The dielectric material is silica with a refractive index of 1.5. All these nanoshell structures are embedded in air and evolve into a linear chain waveguide as depicted in Fig. 1. For structure #1, namely, for the solid silver particle with radius $r_1=20$ nm, the resonance peak was found at a wavelength of 343 nm, as shown in Fig. 2(a). This value agrees very well with the result predicted by the analytic solution [9]. It is worth noting that a further increase of the particle radius r_1 does not provide any significant red shift of the resonance wavelength unless the host medium is altered. For ex-

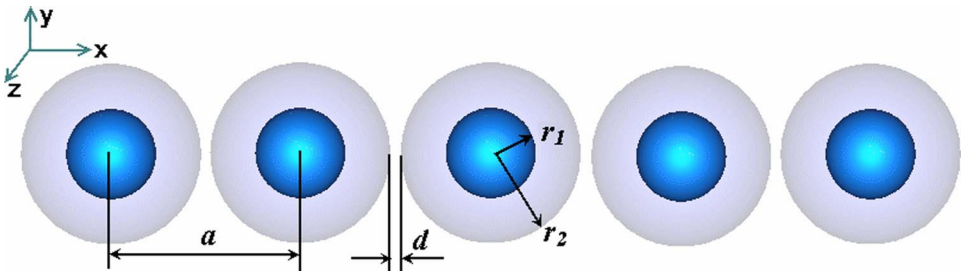

Fig. 1. (Color online) Schematic drawing of a finite nanoshell chain waveguide with constant separation between neighboring particles. The coordinate system and the parameters used in the calculations are also indicated, where a is the center-to-center distance between the nanoshells, d is the interparticle distance, r_1 is the core radius, and r_2–r_1 is the shell thickness. The materials for the core and shell are dielectric and metal or vice versa.

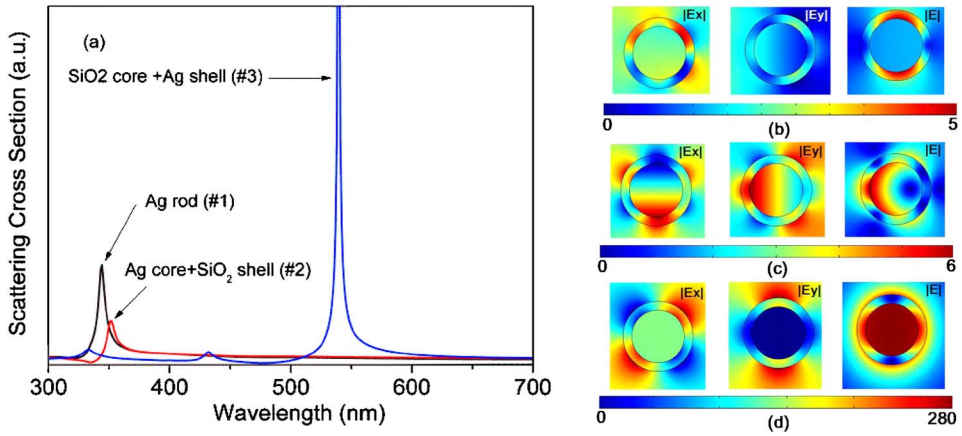

Fig. 2. (Color online) (a) Spectral response of the SCSs of different 2D particle structures; (b)–(d) electric field distributions for the metallic nanoshell (structure #3) with $r_1=15$ nm and $r_2=20$ nm [cf. blue curve in (a)] at the three resonance wavelengths (b) 333 nm, (c) 432 nm; and (d) 539 nm. The grayscale bar (color online) shown in the figure quantifies the field enhancement factor, which is defined as the ratio of the obtained maximal field strength to the incident field.

ample, in order to shift the resonance to telecommunication wavelengths (1550 nm), the permittivity of the surrounding medium has to achieve values up to 50, which is hardly practical. For structure #2, the parameters of the nanoshell are chosen as $r_1=15$ nm, $r_2=20$ nm and a single resonance peak is found at 351 nm. For further variations of the inner radius r_1, small resonance shifts are found, but no additional resonance peak becomes evident in the wavelength range of interest.

In contrast to structure #1 and structure #2, the situation is different for structure #3 when r_1 and r_2 are 15 nm and 20 nm, respectively. The spectral response of the SCS displays three resonances at 333 nm, 432 nm, and 539 nm. The spectral peaks at 333 nm and 432 nm are characterized as multipolar resonances, while the peak at 539 nm is characterized as dipole resonance. Corresponding field distributions for these three resonances are indicated in Figs. 2(b)–2(d). As can be seen, the field distributions at those resonances for structure #3 show a mixing of the plasmon modes on the inner and the outer metal surfaces, namely, the hybridization of the void plasmon and the associated LSP.

Taking advantage of variable geometries and mode hybridization, metallic nanoshells can provide large tuning ranges for SPRs, spanning from the visible wavelength range to the mid-infrared even for a simple two-layered nanoshell sphere [10,11]. Structure #3 is therefore the ideal building block for setting up the corresponding chain waveguide, as we will address in the following sections. It should be noted that the above simulations agree very well with the results predicted by the analytical solutions [9] and typical deviations hover around 1% compared to the exact resonance wavelengths of the SPRs.

B. Transmission Properties of Nanoshell Chains

In this section, we investigate the transmission properties of chain waveguides made of metallic nanoshells (structure #3) as deduced from the previous section. One commonly used approach for evaluating the transmission properties of a chain waveguide is to use the SNOM tip to drive the first particle at the near end of the chain [17,19]. The energy transport in the chain is then realized by the field coupling between the modes of the neighboring particles [19]. The propagation length is determined based on the energy decay within the particle chain. In this paper, we will focus mainly on the cases when the chains are driven at the resonances of an isolated nanoshell. As a first step, we investigate the structural resonances for the chain waveguides with different numbers N of metallic nanoshells. The chain waveguide shown in Fig. 1 with a linear array of metallic nanoshells was then analyzed under plane-wave excitation. The SCS of the overall chain structure is spectrally resolved in Fig. 3 for different chain lengths, i.e., for different numbers of nanoshells and for two different interparticle distances. From the SCS spectra shown in Fig. 3 we can observe that the mesoscopic nature of the finite chain waveguide is clearly visible, as the structural resonances dramatically change with the increase of the chain length, e.g., compared to the resonances of an isolated nanoshell ($N=1$).

Increased field enhancement factors in the chain structure were estimated from their SCSs, which tend to be much larger than the SCS of the underlying single nanoshell at its SPR [9]. Interestingly, some of the resonances of the chain structure remained nearly unchanged; i.e., they shift only within a range of 1 nm when increasing the number of nanoshells. These resonances almost correspond to the SPR of the isolated nanoshell, such as, e.g., the one at 333 nm [as shown in Fig. 2(b)], which is then identified as a high-order multipolar resonance, proving that these high-order resonances are not sensitive to the structure lengths of our chain waveguides.

Recent research shows that the power distributions in finite particle chains exhibit a strong variation on length scales much smaller than the excitation wavelength [20]. Even a short nanoparticle chain can display a complete change in the direction of light scattering when a small detuning is applied to the excitation field [20]. In the context of a finite linear particle array this can sum up to the redirection of the energy flow that is additionally enhanced due to retardation effects. Interference effects at the near and far ends of the finite chain waveguide complicate the picture even further. It is thus worth empha-

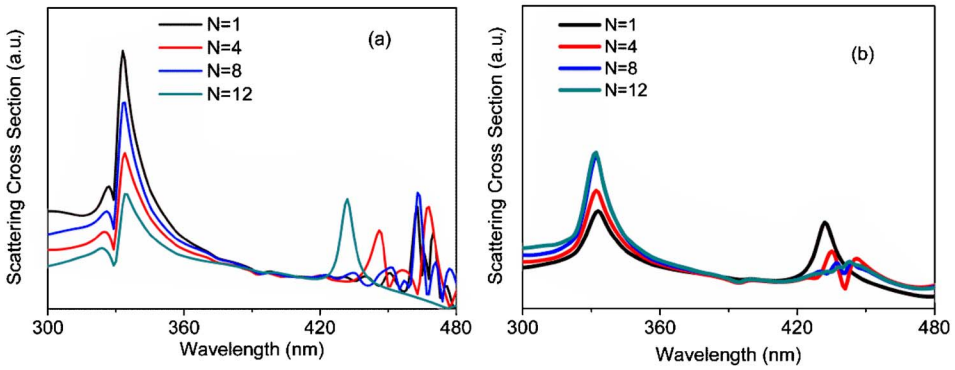

Fig. 3. (Color online) Simulated spectral response of the SCSs for different linear arrays of nanoshell particles ($r_1=15$ nm, $r_2=20$ nm) in air. (a) Arrays consisting of 4, 8, and 12 nanoshells spaced by 2 nm; (b) arrays with 4, 8, and 12 nanoshells spaced by 10 nm. A spectrum for a single nanoshell particle is also shown in each panel. Note that for graphic reasons, only the data from 300 nm to 480 nm were displayed in the figures.

sizing that there is a fundamental difficulty in extracting propagation parameters (such as the propagation constant or the propagation length), especially from resonant finite particle chains, where the length will be always limited by, e.g., the numerical tractability of the underlying problem. When tackling such unavoidable context dependences, proper choices (i.e., number of particles, excitation schemes, etc.) become essential. Our analysis of the loss mechanisms in nanoshell chains has therefore relied on fixed excitation wavelengths that coincide with the corresponding single-particle resonances, where its modal pattern has been impinged on the first particle in the chain irrespective the topology of the subsequent chain.

Besides the metallic nanoshell structure we investigated here, we also found that the chain waveguides containing nanoshells with a metallic core and a dielectric coating (structure #2) are not sensitive to the structure length, even when the energy transmission is supported by low-order (dipole) modes (results not shown here). These findings greatly simplify the experimental procedures, as well as the numerical simulations, i.e., wavelength tuning, etc. Here we will focus only on structure #3, which consists of a dielectric core and a metallic shell.

After investigating the resonant signatures of the particle chain, we start to determine the propagation loss (or propagation length) in the chain waveguides with respect to the different mode coupling mechanisms. As mentioned before, the structures under investigation are driven by the resonant mode patterns of the underlying nanoshell, which is then applied to the first particle in the chain. Linear chains with seven nanoshells are considered throughout this section. In order to examine the attenuation behavior, we analyze the total field intensity $|\boldsymbol{E}|^2$ along the linear chain when excited by a dipole source for L and T polarization, respectively. The dipole is put at 50 nm apart from the center of the first nanoshell of the chain. The obtained intensity values are then averaged and fitted in a log scale plot to extract the propagation loss, referring to the Beer–Lambert law for the field intensity $|\boldsymbol{E}|^2 \times \exp(-\alpha x)$, where x stands for the distance along the propagation axis and α is the power attenuation factor with units of nm^{-1}. The first and last nanoshells are excluded in the calculation in order to mask out the interference effects stemming from impedance mismatch at the near and far ends of the finite chain waveguide [5].

The normalized total field intensity distributions along a seven-nanoshell chain for two different interparticle spacings are shown in Fig. 4, where the origin of the plot is taken in the center of the second nanoshell and extends to the center of the fifth nanoshell. The chain is operated

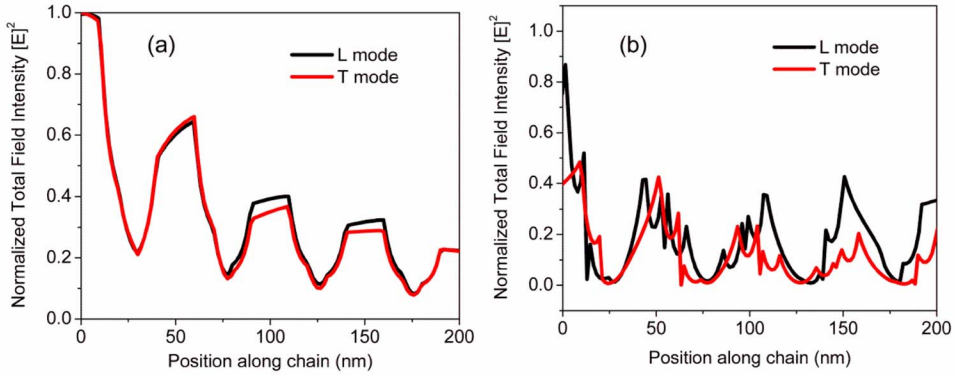

Fig. 4. (Color online) Normalized total field intensity $|\boldsymbol{E}|^2$ along a linear chain with seven nanoshells under transversely (T) and longitudinally (L) polarized excitations when the structure is operated at the single nanoshell resonance (539 nm). (a) For an interparticle separation of 10 nm, and (b) for a reduced interparticle separation of 2 nm. The data were gathered starting from the center of the second nanoshell to the center of the sixth nanoshell in order to mask out potential interference effects at the near and the far ends of the waveguide chain.

at the wavelength of the single nanoshell's dipole resonance (539 nm). The power attenuation factors of the chain waveguide with 10 nm interparticle spacing for L and T waves are 0.0042 nm^{-1} and 0.0043 nm^{-1}, respectively. For the case of 2 nm interparticle spacing [Fig. 4(b)], smaller attenuation factors are found, i.e., 0.0025 nm^{-1} and 0.0030 nm^{-1} for L and T waves, respectively. The two figures [Figs. 4(a) and 4(b)] indicate that the field intensity decays exponentially along the chain; however, it is not trivial to retrieve the propagation loss from such decay when the waveguide's nanoshells are operated at their dipole resonances. This is due mainly to the strong coupling between adjacent dipole fields, where small changes in the chain structure would lead to remarkable variation of the resonance. This phenomenon is typically verified in wire antenna arrays at microwave frequencies when strong coupling is present between neighboring elements.

As shown in Fig. 2, high-order multipolar modes (i.e., at 333 nm and 432 nm for structure #3) exhibit relatively small SCSs, which are thus associated to small field enhancement factors. High-order multipolar modes are therefore mostly ignored in many nanoscale applications due to the presence of dominant dipole modes. However, our previous investigations have revealed that some high-order multipolar modes are less sensitive to the structure length and display, promising far-field characteristics [10]. It is thus worth examining the transmission properties based on multipolar excitations using, e.g., the SPR of the single nanoshell at 333 nm (cf. Fig. 2) as an excitation field to drive the first particle in the nanoshell chain. Figure 5 depicts the distribution of the normalized total field intensity along the chain at this resonance wavelength. The field is well confined along the surfaces of nanoshells, and an exponential decay of the intensity is clearly observed. Figure 5 also shows that, despite the field intensity of the high-order multipolar mode being smaller than

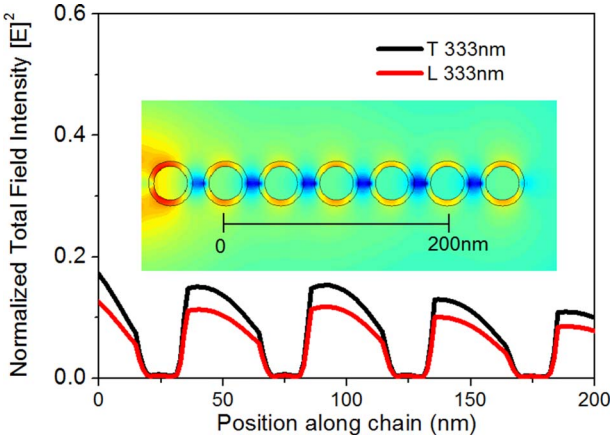

Fig. 5. (Color online) Normalized total field intensity $|\boldsymbol{E}|^2$ along a linear chain with seven nanoshells under transverse (T) and longitudinally (L) polarized excitation when the structure is operated at the single nanoshell's multipolar resonance wavelength of 333 nm. The data were taken from the center of the second nanoshell to the center of the sixth nanoshell (as indicated by the scale bar inset) in order to mask out potential interference effects at the near and the far ends of the waveguide chain. The interparticle distance is 10 nm. Inset: Total field intensity distribution for transverse polarization (T mode).

that of the low-order mode displayed in Fig. 4(a), significantly smaller attenuation factors, such as 0.00057 nm^{-1} for the T wave and 0.00053 nm^{-1} for the L wave, are found, where the latter two values correspond to a $1/e$ propagation length of 1.75 μm and 1.88 μm, respectively.

Up to now we have focused on the cases where the chain waveguides were operated at the resonances of the single nanoshell, where very tight field confinement with correspondingly larger propagation loss is observed. It is well known that subwavelength nanoparticles will at first respond as dipoles to an impinging optical field regardless of their resonant states [9]. Therefore, off-resonant wave guiding in the chain structure can also be modeled as simple dipole–dipole interactions between the neighboring nanoshells. Compared to the resonant case, the internal damping of the plasmon oscillation becomes negligible and only radiation loss of the overall structure has to be taken into account. When the number of particles is increased to some extent (while keeping the interparticle distance constant), the energy propagation is then predominantly realized by the radiative interactions among the nanoparticles [20]. In order to provide a phenomenology to this consideration, we selected several excitation wavelengths and plotted the total field intensity distributions along the chain waveguides as displayed in Fig. 6(a) for T-wave excitation. As expected, all the off-resonant field distributions look conceptually similar; for instance, all the local fields inside the nanoshells oscillate coherently perpendicular to the chain axis, and the fields display small attenuations after experiencing a certain propagation distance. A small damping factor $\alpha = 0.000897\ nm^{-1}$ was observed at a wavelength of 500 nm, which corresponds to a $1/e$ propagation length of approximately 1.1 μm. Since the field confinement in the off-resonant chain waveguide is less tight (i.e., the mode confinement area is two times larger than that of the resonant case) than in the resonant case (where the energy flow in a typical near-field region of 10 nm tends to be directed toward the metallic coating [9]), the corresponding energy flow extends along the whole chain structure, suffering only from slight perturbations by the underlying particles. Thus, the trade-off between field confinement and propagation lengths that is generally observed in continuous plasmon guides seems to hold also for chain waveguides. Besides the apparent field confinement, there is also evidence for pronounced interference effects at the waveguide's far end, as indicated in Fig. 6. It should be noted that far-field effects may play an important role in both the resonant and the off-resonance cases with increasing structure length, especially when the structure is larger than the incident wavelength. For example, the energy flow in the structure can be redirected even within a very short chain [21]. In this case, it is difficult to determine the transmission loss either by numerical or experimental methods.

C. Loss Reduction in Chain Waveguide Structures

In principle, there is no essential difference between nanoshell structures and solid metallic rods when they are employed to form chain waveguides based on the near-field coupling of neighboring particles. Nevertheless, it is worth examining the loss reduction mechanisms in

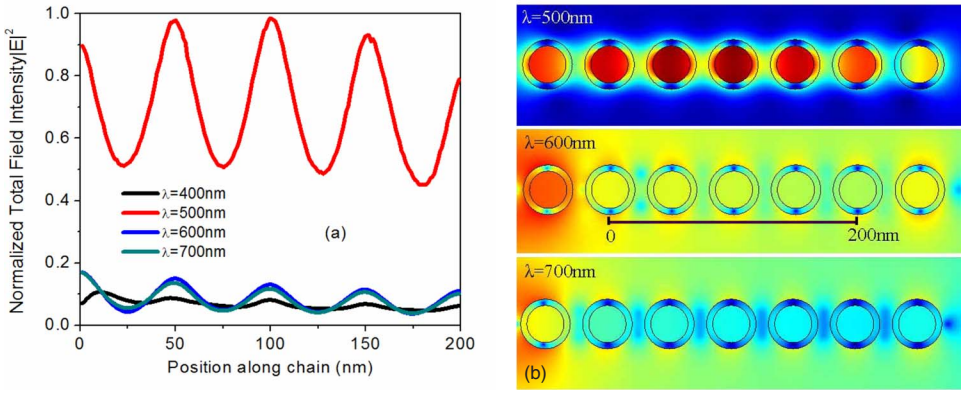

Fig. 6. (Color online) Normalized total field intensity $|\boldsymbol{E}|^2$ along a linear chain with seven nanoshells having an interparticle distance of 10 nm under T polarization when the structure is operated at wavelengths that are considerably detuned from the single nanoshell resonances. (a) Total field intensity distribution along the black curve as indicated in (b), where in the scale bar inset, "0" indicates the starting point of the plot position in (a); (b) corresponding total field intensity distributions for different wavelengths.

our structures, since our results show that the propagation losses in the nanoshell chain waveguides can be much smaller than those of solid metallic particles [22]. First, the near-field distributions of isolated nanoparticles are investigated by plotting the total fields across the centers of particles (Fig. 7), where the field enhancement is derived as the ratio of the total field to the incident field. Figure 7(a) depicts the field enhancement along both the x and the y directions for the analyzed nanoshell at a dipole resonance wavelength of 539 nm. As observed in Fig. 7(a), the field is concentrated mainly in the core region and strongly decays toward the outer region. This also holds for the case of the solid metallic particle with the same volume [$r_1 = 20$ nm, Fig. 7(b)]. However, as indicated in Figs. 7(a) and 7(b), the field enhancement for the nanoshell operated at the dipole resonance is twice as large when compared to the solid metallic particle. This is attributed to the large coupling between the plasmons of the two metal–dielectric interfaces (i.e., to the hybridization of the two localized SP types), leading to a significantly larger field enhancement.

Therefore, one of the loss reduction mechanisms in nanoshell chain waveguides is probably due to the fact that the metallic shells enhance the field in the interparticle space, increasing the coupling between the nanoshells. This conclusion is additionally supported by recent experiments [23]: There a chain waveguide was interfaced with a condenser, where the high-intensity focus of the condenser was placed in the vicinity of the waveguide input in order to excite the aforementioned modal fields, thus enabling an improved energy transport.

For the case of high-order mode coupling, we plot the field distribution of an isolated nanoshell at its multipolar resonance wavelength of 333 nm [Fig. 7(c)]. In contrast to the previous cases [Figs. 7(b) and 7(c)], the field enhancement is much smaller and the field strength along the propagation direction (i.e., the x direction) is significantly lower than along the y direction. This, however, shows that the total multipolar moment is perpendicular to the chain axis (x). Earlier investigations of nanoshell structures have shown [10] that for multipolar modes, light scattering occurs predominantly in the forward direction, providing stronger foci if the incident light is p polarized. Hence, the multipolar moment can strongly interact with the field of the scattered light from the neighboring nanoshells, which inherently leads to an increase in the propagation length, since the far-field coupling starts to dominate the field behaviors [21,22].

Besides the aforementioned loss reduction mechanisms, from Fig. 7 we can also deduce that the field confinement in the metallic regions will inevitably result in high absorption losses. Therefore, a reduced field confinement in the metallic region will inevitably lead to lower absorption in the nanoshells. An additional loss reduction can be achieved if nanoshells with elongated shapes are used [5]. This so-called nanorice design would carry significant potential for low-loss nanoshell chain waveguides [24]. Due to the high absorption loss in metals at optical frequency, it is better to employ such modified chain structures because they are prone to larger resonance wavelengths, typically in the near infrared, where less absorption is expected.

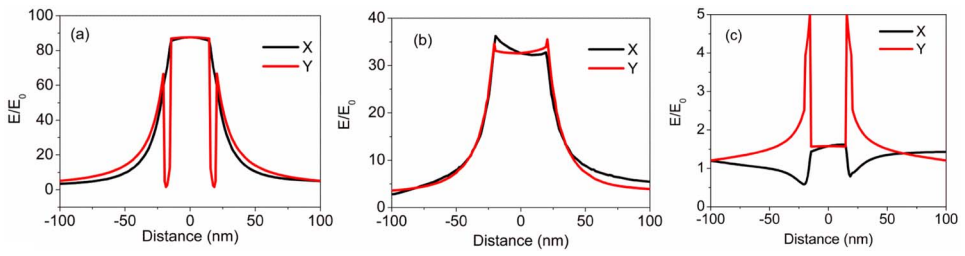

Fig. 7. (Color online) Simulation of the total electric field distribution at resonance, showing the near-field enhancement along the different particle's cross section. (a) Nanoshell at a resonance wavelength of 539 nm (dipole resonance), (b) solid metallic rod at 341 nm, (c) nanoshell at the multipolar resonance wavelength of 333 nm.

4. SUMMARY

Plasmonic waveguides based on periodic linear arrays of nanoshells embedded in air are investigated for efficient light confinement and light guiding in the nanoscale. The analysis was performed using numerical FEM analysis that can handle highly dispersive materials and complex geometries. Because of the large tunability of the nanoshells, our chain waveguide can be easily tailored for different operation wavelengths, ranging from ultraviolet to near infrared. We found that the resonances of the finite chain waveguide formed by nanoshells are less sensitive to the waveguide length when operated on the nanoshell's multipolar resonances. The propagation losses of the chain waveguide are evaluated at different excitation modes and excitation polarizations. Our results show that large propagation distances in resonant chain waveguides are usually associated with a large field enhancement between the nanoshells, which enhances the mode coupling and thus lowers the insertion losses.

REFERENCES

1. W. L. Barnes, A. Dereux, and T. W. Ebbesen, "Surface plasmon subwavelength optics," Nature **424**, 824–830 (2003).
2. P. Berini, "Plasmon-polariton waves guided by thin lossy metal films of finite width: Bound modes of symmetric structures," Phys. Rev. B **61**, 10484 (2000).
3. J. R. Krenn, B. Lamprecht, H. Ditlbacher, G. Schider, M. Aalerno, A. Leitner, and F. R. Aussenegg, "Non-diffraction-limited light transport by gold nanowires," Europhys. Lett. **60**, 663–669 (2002).
4. E. Moreno, S. G. Rodrigo, S. I. Bozhevolnyi, L. M. Moreno, and F. J. G. Vidal, "Guiding and focusing of electromagnetic fields with wedge plasmon polaritons," Phys. Rev. Lett. **100**, 023901 (2008).
5. M. Quinten, A. Leitner, J. R. Krenn, and F. R. Aussenegg, "Electromagnetic energy transport via linear chains of silver nanoparticles," Opt. Lett. **23**, 1331–1333 (1999).
6. M. L. Brongersma, J. W. Hartman, and H. A. Atwater, "Electromagnetic energy transfer and switching in nanoparticle chain arrays below the diffraction limit," Phys. Rev. B **62**, 16356–16359 (2000).
7. L. A. Sweatlock, S. A. Maier, H. A. Atwater, J. J. Penninkhof, and A. Polman, "Highly confined electromagnetic fields in arrays of strongly coupled Ag nanoparticles," Phys. Rev. B **71**, 235408 (2005).
8. S. A. Maier and H. A. Atwater, "Plasmonics: Localization and guiding of electromagnetic energy in metal/dielectric structures," J. Appl. Phys. **98**, 011101 (2005).
9. U. Kreibig and M. Vollmer, *Optical Properties of Metal Clusters* (Springer-Verlag, 1995).
10. S. J. Oldenburg, G. D. Hale, J. B. Jackson, and N. J. Halas, "Light scattering from dipole and quadrupole nanoshell antennas," Appl. Phys. Lett. **75**, 1063–1065 (1999).
11. P. Alivisatos, "The use of nanocrystals in biological detection," Nat. Biotechnol. **22**, 47–52 (2004).
12. N. C. Panoiu and R. M. Osgood, Jr., "Linear and nonlinear transmission of surface plasmon polaritons in an optical nanowire," in *Organic and Nanocomposite Optical Materials*, Vol. 846 of the MRS Symposium Proceedings Series, A. Cartwright, T. M. Cooper, S. P. Karna, and H. Nakonishi, eds. (Materials Research Society, 2005), pp. DD5.6.1–DD5.6.6.
13. J. L. West and N. J. Halas, "Engineered nanomaterials for biophotonics applications: Improving, sensing, imaging, and therapeutics," Annu. Rev. Biomed. Eng. **5**, 285–294 (2003).
14. COMSOL Multiphysics (Version 3.3) is a FEM-based multipurpose simulation platform, available at http://www.comsol.com.
15. P. B. Johnson and R. W. Christy, "Optical constants of the noble metals," Phys. Rev. B **6**, 4370 (1972).
16. A. Downes and Ph. Dumas, "Chemical analysis and optical properties of metallic nanoclusters," Appl. Surf. Sci. **770**, 212–213 (2003).
17. H. Ditlbacher, J. R. Krenn, G. Schider, A. Leitner, and F. R. Aussenegg, "Two-dimensional optics with surface plasmon polaritons," Appl. Phys. Lett. **81**, 1762–1764 (2002).
18. B. S. Hwang, M. H. Kwon, and J. Kim, "Use of a near field optical probe to locally launch surface plasmon polaritons on plasmonic waveguides: A study by the finite difference time domain method," Microsc. Res. Tech. **64**, 453–458 (2004).
19. S. A. Maier, P. G. Kik, H. A. Atwater, S. Meltzer, E. Harel, B. E. Koel, and A. A. G. Requicha, "Local detection of electromagnetic energy transport below the diffraction limit in metal nanoparticle plasmon waveguide," Nat. Mater. **2**, 229–232 (2003).
20. R. D. Waele, A. F. Koenderink, and A. Polman, "Tunable nanoscale localization of energy on plasmon particle arrays," Nano Lett. **7**, 2004–2008 (2007).
21. J. V. Hernandez, L. D. Noordam, and F. Robicheaux, "Asymmetric response in a line of optically driven metallic nanospheres," J. Phys. Chem. B **109**, 15808–15811 (2005).
22. S. A. Maier, P. G. Kik, and H. A. Atwater, "Observation of coupled plasmon-polariton modes in Au nanoparticle chain waveguides of different lengths: Estimation of waveguide loss," Appl. Phys. Lett. **81**, 1714–1716 (2002).
23. W. Nomura, M. Ohtsu, and T. Yatsui, "Nanodot coupler with a surface plasmon polariton condenser for optical far/near-field conversion," Appl. Phys. Lett. **86**, 181108 (2005).
24. H. Wang, D. W. Brandl, F. Lei, P. Nordlander, and N. J. Halas, "Nanorice: A hybrid plasmonic nanostructure," Nano Lett. **6**, 827–832 (2006).